Role of Solvent Rearrangement on Mg^{2+} Solvation Structures in Dimethoxyethane Solutions using Multimodal NMR Analysis

Ying Chen[a,b], Nicholas R. Jaegers[a], Hui Wang[a,b], Kee Sung Han[a,b], Jian Zhi Hu[a,b], Karl T. Mueller[a,b]* and Vijayakumar Murugesan[a,b]*

[a] Physical and Computational Sciences Directorate, Pacific Northwest National Laboratory, Richland, Washington 99352, United States

[b] Joint Center for Energy Storage Research (JCESR), Lemont, Illinois 60439, United States

*To whom correspondence should be made

Vijay@pnnl.gov; (509) 371-6540

Karl.Mueller@pnnl.gov; (509) 371-6550.

Table of contents:

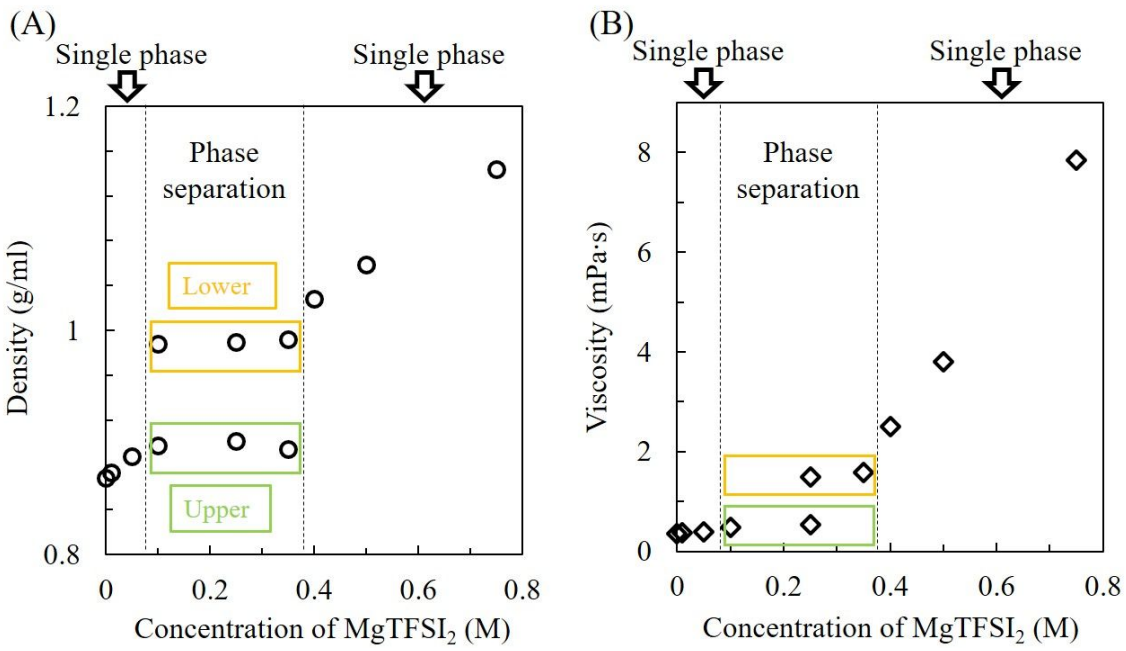

Figure S1. Density (A) and viscosity (B) of $MgTFSI_2$/DME solutions measured at 25 °C. The data points of the 0.1 M lower phase and 0.35 M upper phase are missing from (B) because these two layers do not produce enough solutions for accurate viscosity measurement in our instrument. We also prepared solutions at 1.0 M and 1.25 M, but their data are not reported here as they do not maintain as clear liquids during the experimental conditions that we employed during our NMR measurements (between -10 and 30 °C). The 1.25 M solution nucleates easily with a slight perturbation at room temperature, while the 1.0 M solution nucleates below 5 °C.

Apparent molar volume ${}^{\varphi}V_2$ of $MgTFSI_2$ in DME is calculated using the density of pure DME ρ_1^* (g/ml), the density of the solution ρ (g/ml), the molar concentration c_2 (mol/L), and the molar mass of $MgTFSI_2$ M_2 (g/mol):

$$^{\varphi}V_2 = M_2/\rho_1^* + 1000(\rho_1^* - \rho)/\rho_1^* c_2$$

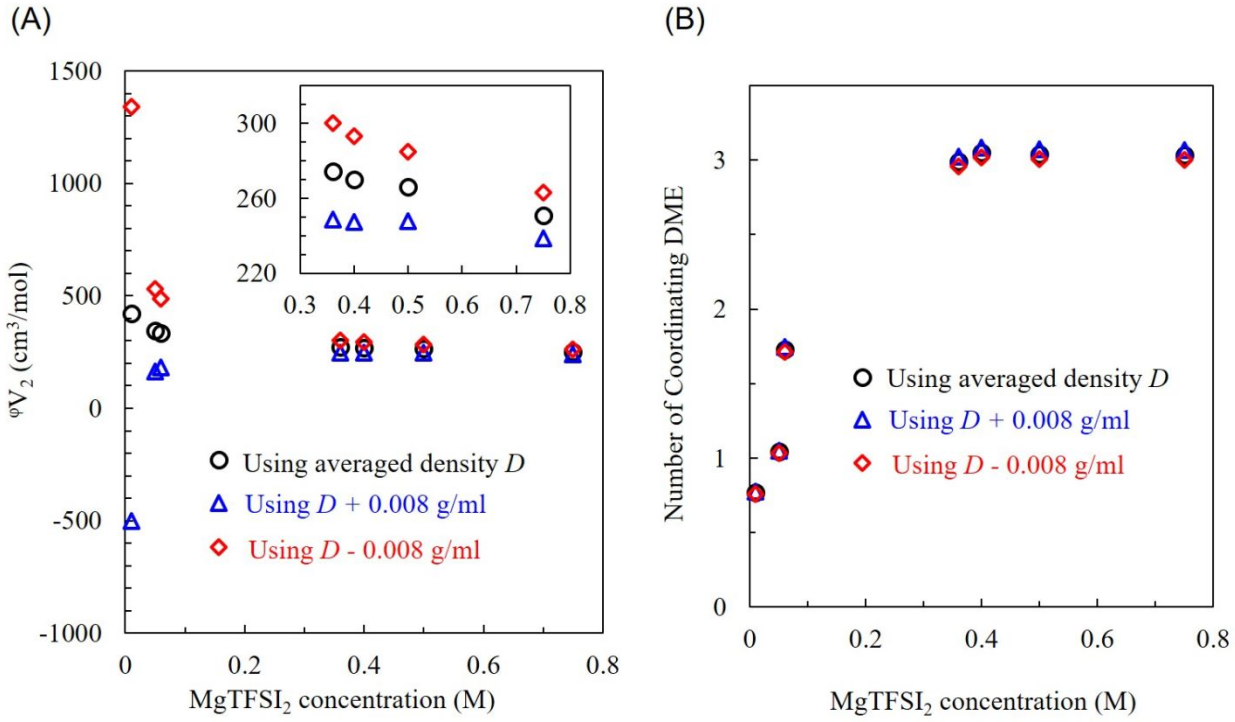

Figure S2. (A) Apparent molar volume ${}^{\varphi}V_2$ vs salt concentration. The experimental error in density ± 0.008 g/ml leads to a dramatic deviation in calculated ${}^{\varphi}V_2$ values especially at lower concentrations (≤ 0.06 M). (B) Number of coordinating DME vs salt concentration shows that the same error in density (± 0.008 g/ml) does not affect the calculated coordinating number. The main error of the DME coordinating number comes from the fraction of bound DME obtained via ^1H NMR.

Experimental Methods

Sample preparation: $Mg(TFSI)_2$ (99.5%, Solvionic) were dried for two days under vacuum at 180 °C prior to usage. The DME solvent (Battery-grade, Gotion) was further dried over activated 3Å molecular sieves in a glovebox until its moisture content was determined to be below 10 ppm using a Karl-Fisher Titrator (Metrohm). $Mg(TFSI)_2$/DME solutions were prepared inside a glovebox filled with Argon right before NMR measurements, with the water content measured to be around 7 – 9 ppm using the Karl-Fisher Titrator. The density at 20 °C was measured inside the glove box with the blow rate set to the minimum by using the mass of 500 µL solution from a 1 mL pipette or 100 µL solution from a 200 µL pipette. Each solution was measured three times and an average value was reported. To estimate the density and morality of $MgTFSI_2$/DME solutions at different temperatures, we placed 1 mL solution inside a NMR tube, marked the height of the solution, placed it inside a NMR instrument at temperatures ranging from – 9 °C to 30 °C for 30 min, injected the tube, marked the change in the solution height, and calculated density and morality based on the change in the solution volume. We understand that the error related to these density measurements is high compared to the more accurate density determinations by pycnometry or vibrating tube densimeters, but the accuracy in density (± 0.008 g/ml) is enough for our calculations to obtain molarity of DME and number of coordinating DME as shown in Figure 2 and Figure S2.

^{1}H, ^{19}F, ^{25}Mg and ^{17}O NMR: As shown in Figure S3, to record the exact ^{1}H and ^{19}F chemical shift of $MgTFSI_2$/DME solution, a coaxial NMR tube (12.4 µL/cm) was used to hold the sample while 1 v/v% CF_3COOH and 0.1 % H_2O in D_2O (99.9%, from Sigma Aldrich) placed in the outer NMR tube served as external ^{19}F and ^{1}H NMR reference at -76.55 ppm and 4.77 ppm, respectively. For less sensitive ^{17}O and ^{25}Mg, a thin-wall 5 mm NMR tube was employed to hold more sample (159

μL/cm). In order to minimize the spectrometer drift effect on chemical shift, D_2O and 5 M $MgCl_2$ were used to set 0 ppm for ^{17}O and ^{25}Mg, respectively, right before each NMR measurement. For variable-temperature measurements, the sample was equilibrated at each temperature for 20 minutes prior to each NMR experiment.

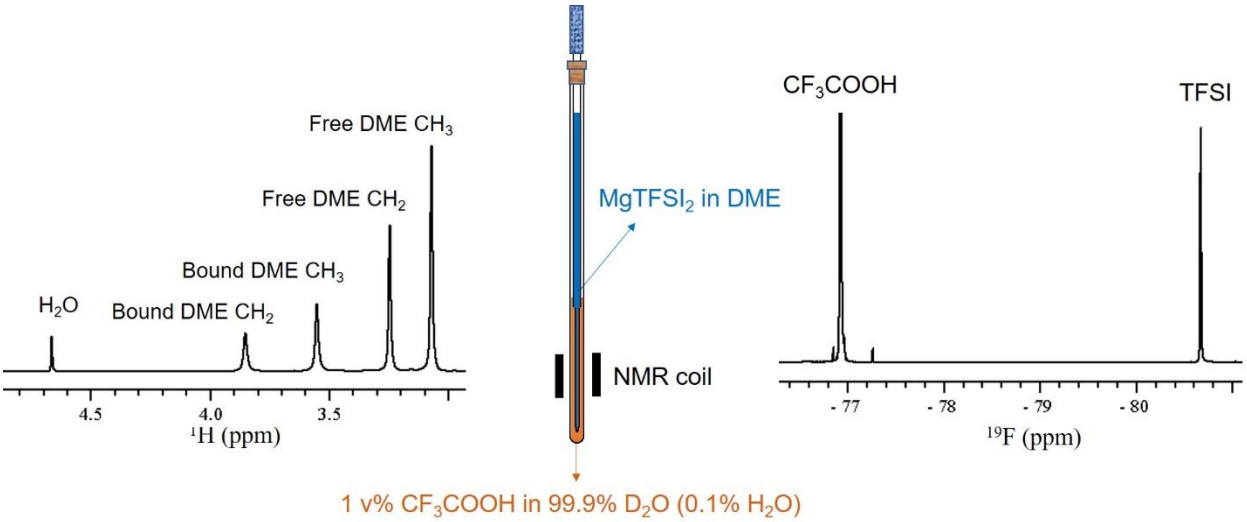

Figure S3. The experimental setup with a coaxial insert holding $MgTFSI_2$/DME solution and an outer thin-wall NMR tube hosting 1 v% CF_3COOH (as the ^{19}F reference) and 0.1 v% H_2O (as the ^{1}H reference) in D_2O (for signal lock).

^{1}H and ^{17}O NMR measurements were performed on a Varian DDRS spectrometer with a 17.6 T magnet using a broad-band (BBO) probe with ^{1}H and ^{17}O Larmor frequencies of 748.1 and 101.4 MHz, respectively. The 90˚ pulse widths were 20 μs for ^{1}H and 23 μs for ^{17}O. For obtaining exact chemical shift values, ^{1}H spectra were collected using 90° pulses with a transition number of 16 and a recycle delay of 20 s. For obtaining quantitative integration ratios of bound DME to free DME, requiring smooth baselines, ^{1}H spectra were collected using a small tip angle of 3° with a recycling delay of 5 s and with the number of averaged acquisitions varying from 64 to 2400 depending on solution concentration. For obtaining quantitative integration ratios of DME to TFSI,

^{17}O spectra were collected by setting the carrier frequency halfway between the two peaks and using a small tip angle of 15° with a recycling delay of 0.1 s and a with the number of averaged acquisitions varying from 128,000 to 2,560,000 depending on solution concentration.

^{19}F and ^{25}Mg NMR spectra were collected on a Varian DDR spectrometer with a 14.1 T magnet using a DOTY diffusion probe with ^{19}F and ^{25}Mg Larmor frequencies of 564.7 and 36.7 MHz, respectively. The 90° pulse widths were 12 μs for ^{19}F and 20 μs for ^{25}Mg.

T_1 and T_2 relaxation time constants were measured using inversion-recovery and CPMG methods, respectively. TFSI diffusion coefficient were measured using bipolar pulse pair stimulated echo pulse sequences "Dbppste" and "Dbppste_cc" with convection compensation on the coaxial tube setup to further reduce convention effects at different temperatures. The typical parameters for ^{1}H DOSY experiments were: gradient g = 1.6 – 1200 G/cm, number of increments = 48, diffusion gradient duration δ = 1 ms, diffusion delay Δ = 5 – 1200 ms, gradient stabilization delay = 1 ms, number of scans = 32.

Computational Methods

Density Functional Theory-based NMR chemical shift modeling was carried out using the Amsterdam Density Functional (ADF-2018) package. Cluster geometries were optimized with the generalized gradient approximation (GGA) applied by the Becke-Lee-Yang-Parr functional. Calculations were carried out using the all-electron TZ2P basis set (Triple-ζ, 2-polarization function) with the Slater-type orbitals implemented in the ADF program. NMR calculations were performed based on the geometry-optimized structures at the same level of the theory and with the same basis set to evaluate the chemical shielding for each atom.

As summarized in Figure S3A, ^{1}H chemical shifts of bound CH_2, bound CH_3, free CH_2 and free CH_3 change from 4.32, 4.07, 3.67, and 3.51 ppm at 0.01 M to 4.00, 3.69, 3.38, and 3.21 ppm at 0.75 M, the differences between the chemical shifts are maintained despite the large concentration range, indicating that the change in the chemical shifts versus concentration are mainly caused by magnetic susceptibility, which may also be the reason behind the ^{19}F chemical shift change of TFSI. DFT-NMR calculations of optimized structures (Table S1) show that free DME has the chemical shifts at 3.69 and 3.54 ppm, while the bound DME, the optimized $Mg(DME)_1(TFSI)_1$, $Mg(DME)_2(TFSI)_1$ and $Mg(DME)_3$ produce chemical shifts at 4.12 – 4.37 ppm for CH_2 and 4.00 – 4.03 ppm for CH_3, all close to the experimental values for the bound DME. This implies that ^{1}H chemical shifts of bound DME are not sensitive to the local solvation structure (i.e., whether TFSI is also coordinating to Mg^{2+}), therefore we cannot distinguish these structures using ^{1}H or ^{19}F chemical shifts.

Note that the DFT calculations of ^{1}H and ^{19}F chemical shifts are relatively accurate, especially that the separation between the free and bound DME in ^{1}H chemical shifts are consistent between the experimental values and DFT calculations. However, DFT calculated ^{25}Mg and ^{17}O chemical shifts have significant discrepancies from experimental values, so we only use the changes in different structures to compare with experimental values.

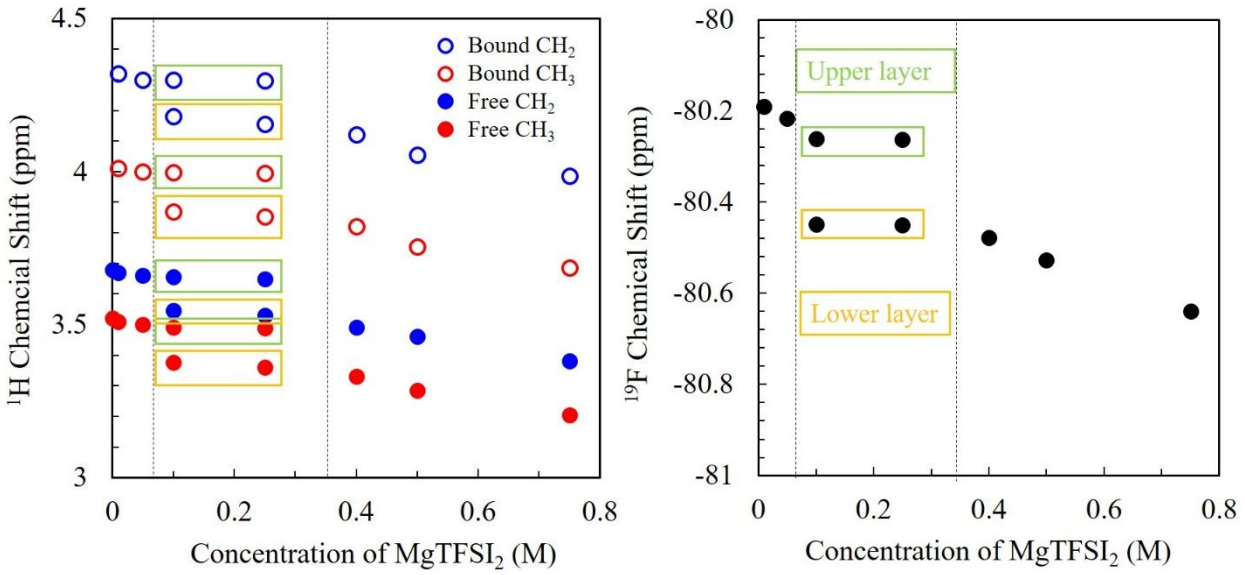

Figure S4. (A) ^{1}H chemical shifts of bound CH_2 (blue open circles), bound CH_3 (red open circles), free CH_2 (blue filled circles) and free CH_3 (red filled circles) of DME and (B) ^{19}F chemical shifts of TFSI in $MgTFSI_2$/DME of varying concentrations at 10 °C.

Table S1. Chemical shifts calculated using DFT-NMR based on optimized structures

Structure	δ ^{1}H	δ ^{19}F	δ ^{17}O	δ ^{25}Mg
TMS 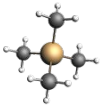	0.12			
2TMS 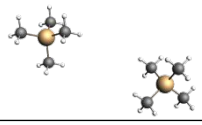	0.12			
2DME 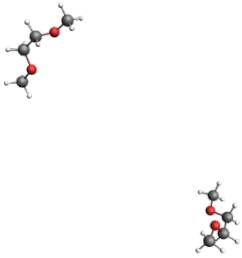	H_2C: 3.69 H_3C: 3.54		-46.995	
CF_3COOH 		-76.55		
$12H_2O$ 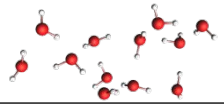	4.89		0	
$Mg^{+}(H_2O)_6$ 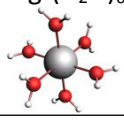			-80.72	0
Mg-2DME 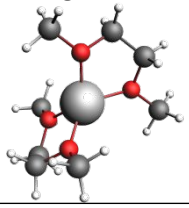	H_2C: 4.52 H_3C: 4.28		-65.23	20.77
Mg-1DME - 1TFSI 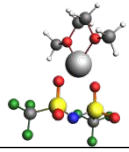	H_2C: 4.37 H_3C: 4.12	-76.16	DME: -63.29 TFSI_Un: 173.26 TFSI_Coord: 109.51 TFSI: 131.385	19.36
Mg-2TFSI 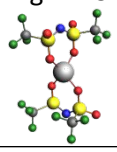		-79.36	125.77	11.79

Mg-2DME - 1TFSI 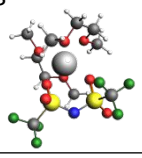	H_2C: 4.08 H_3C: 3.99	-79.70	DME: -59.45 TFSI_Un: 173.46 TFSI_Coord: 109.71 TFSI: 131.59	-4.24
Mg-3DME 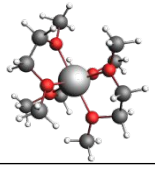	H_2C: 4.25 H_3C: 4.03		-64.2	-4.68
Mg-3DME-TFSI 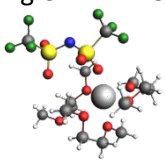	1-H_2C: 4.12 1-H_3C: 4.03 2-H_2C: 4.10 2-H_3C: 4.03	-79.72	TFSI: 147.2175 1-DME: -63.18 2-DME: -60.37	-8.77
Mg-4DME 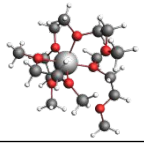	1-H_2C: 4.23 1-H_3C: 3.91 2-H_2C: 4.14 2-H_3C: 4.25		-57.87	-11.25
Mg-4DME-relaxed 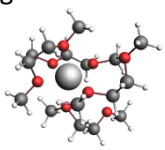	1-H_2C: 4.23 1-H_3C: 3.91 2-H_2C: 4.24 2-H_3C: 4.14		1C: -57.89 2C: -62.05	-11.23

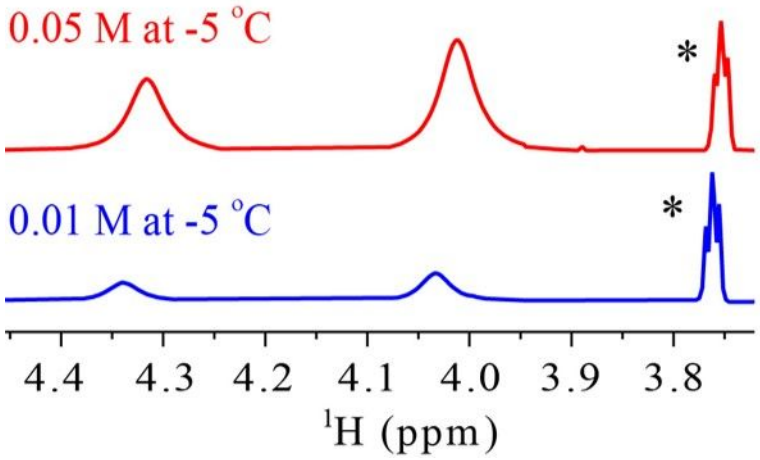

Figure S5. ^{1}H NMR spectra of bound DME and $^{13}CH_2$ satellite peak of free CH_2 (denoted by "*"), the fraction of bound DME can be calculated from the integration ratio of bound CH_2 and the satellite peak.

In order to reduce the error related to calculating the fraction of bound DME by comparing the small signals of bound DME to much greater signals from free DME, we also use the integration ratio (r) of the bound CH_2 peak to the $^{13}CH_2$ satellite peak of the free CH_2 peak (Figure S4):

$$\text{fraction of bound DME} = r/(r + 1/(1.109/2) * 100)$$

^{25}Mg NMR Analysis:

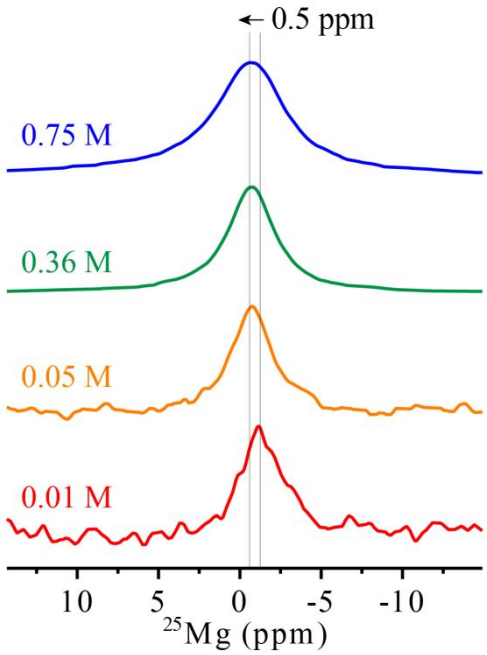

Figure S6. ^{25}Mg NMR spectra of $MgTFSI_2$/DME solutions collected at 10 °C.

As shown in Figure S6, the ^{25}Mg peak position slightly shifts from -0.77 ppm at 0.01 M to -0.27 ppm at 0.75 M. By comparison, DFT calculations (Table S1) predict that ^{25}Mg chemical shifts change from 12 – 21 ppm for four-coordinate clusters $Mg(DME)_2^{2+}$, $Mg(TFSI)_2$, and $Mg(DME)(TFSI)^+$, to -4.6 – -4.2 ppm for six-coordinate clusters $Mg(DME)_3^{2+}$ and $Mg(DME)_2(TFSI)^+$, to -8.8 – -12 ppm for eight-coordinate clusters $Mg(DME)_4^{2+}$, and $Mg(DME)_3(TFSI)^+$. Although there is a significant discrepancy between the calculated chemical shift of -4.68 ppm and the experimental value of -0.77 ppm for $Mg(DME)_3^{2+}$, the trend is clear that a higher coordinating number leads to greater shielding of the Mg^{2+} ions and thereby a more negative chemical shift value. Since we have calculated from quantitative ^{1}H NMR that at higher concentrations (0.36 – 0.75 M), all Mg^{2+} ions are present as fully solvated clusters (i.e., $Mg(DME)_3^{2+}$), the small shift of 0.5 ppm from 0.75 M to 0.01 M suggests that the detected signals

are also from octahedrally coordinated clusters at low concentrations, so that the detectable Mg species in the electrolytes may be $Mg(DME)_3^{2+}$, $Mg(DME)_2(TFSI)^+$, and $Mg(DME)(TFSI)_2$. The spin count from the ^{25}Mg spectra at different concentrations is not accurate enough for us to predict the fraction of undetectable ^{25}Mg signal due to the low signal to noise ratio in ^{25}Mg spectra from 0.01 – 0.05 M.

Dissociative Ligand Exchange Process:

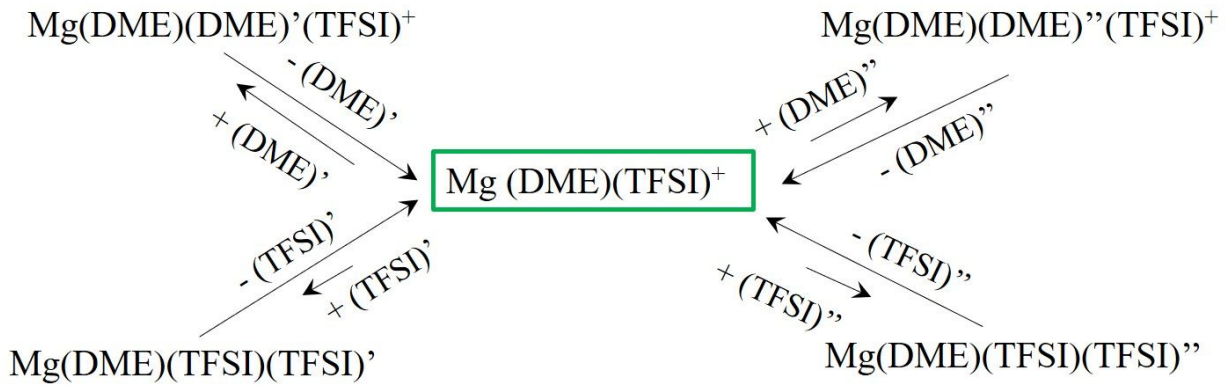

Scheme S1. Proposed dissociative ligand substitution mechanism that could lead to observation of a four-coordinated $[Mg(DME)_1(TFSI)_1]^+$ type cluster with NMR experiments at 0.01 M.

Impurity Analysis:

Inadvertent water present in solution could preferentially coordinate to Mg^{2+} and influence the solvent coordination number derived from NMR analysis. For the as-received DME (Battery-grade, Gotion), the moisture content was about 30 ppm measured by a Karl-Fisher Titrator (Metrohm). In our experiment, $Mg(TFSI)_2$ (99.5%, Solvionic) was dried for two days under vacuum at 180 °C prior to usage, and DME was further dried over activated 3Å molecular sieves in a glovebox. The water content of the final $Mg(TFSI)_2$/DME solutions was around 7 – 9 ppm determined using the Karl-Fisher Titrator. Compared to the smallest fraction of bound DME at 0.01 M (0.0008), the water content was only ~1% of the bound DME, so we posit that it does not influence our NMR based solvation structural analysis. We also perform NMR sample loading in the glove box right before NMR measurements to avoid any further exposure to moisture. Experimentally, ^1H NMR showed no evidence of trace water in the solution. For example, the ^1H NMR of the 0.01M solution (Figure S7) has two impurity peaks representing hydrocarbons, a triplet centered at 6.67 ppm and an even smaller singlet at 1.51 ppm with total spectral fractions of 0.012% and 0.001%, respectively. Even if these impurities could somehow coordinate to Mg^{2+} and lower the DME coordination number, their total fraction is only 1/8 of the bound DME, so it is unlikely to influence our solvation structural analysis.

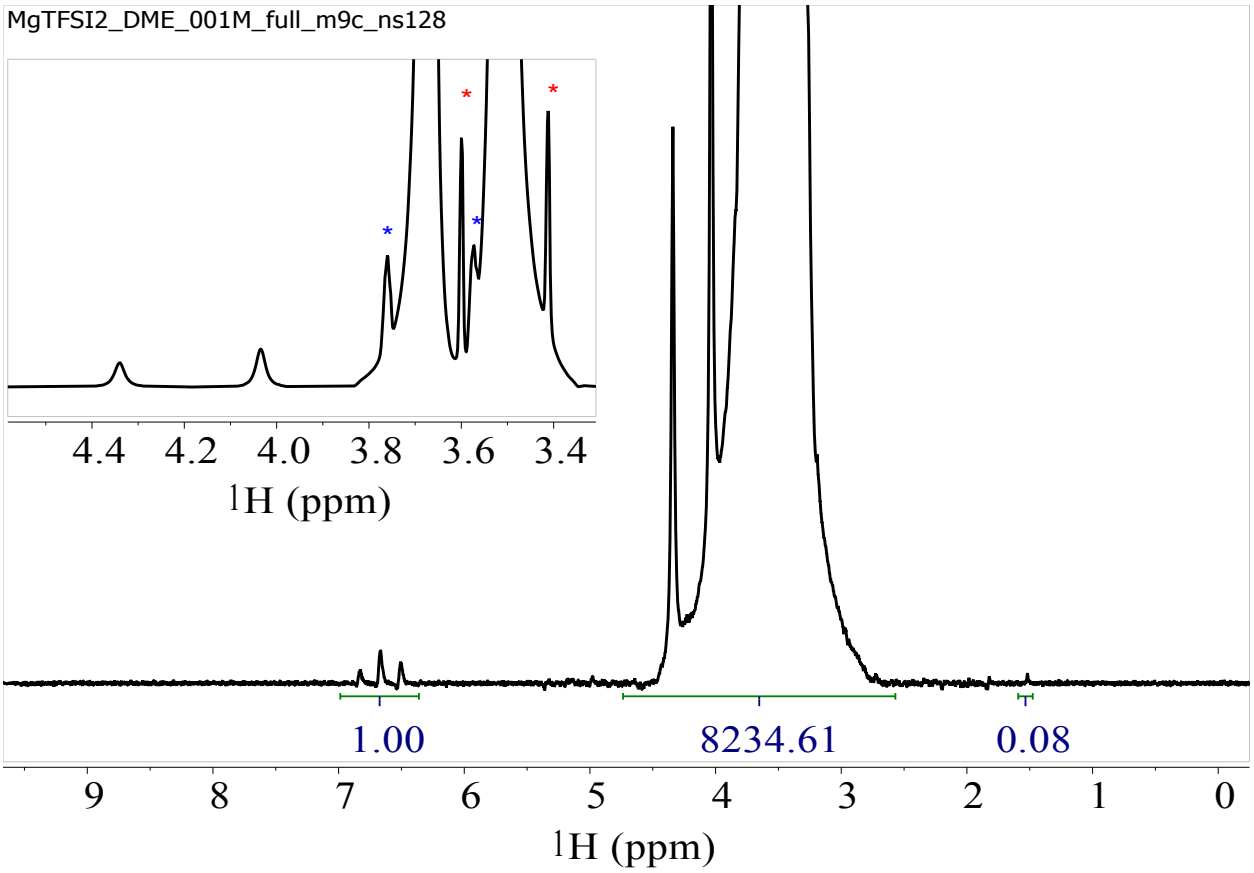

Figure S7. High resolution ^{1}H spectrum of 0.01 M $MgTFSI_2$/DME solution at -9 °C. The blue and red asterisks are the ^{13}C satelites of free DME CH_2 and CH_3 resonances, respectively.